EFDA–JET–PR(11)66

J. Eriksson, C. Hellesen, E. Andersson Sunden, M. Cecconello, S. Conroy,
G. Ericsson, M. Gatu Johnson, S.D. Pinches, S.E. Sharapov,
M. Weiszflog and JET EFDA contributors

Larmor Radii Effects in Fast Ion Measurements with Neutron Emission Spectrometry

Larmor Radii Effects in Fast Ion Measurements with Neutron Emission Spectrometry

J. Eriksson[1], C. Hellesen[1], E. Andersson Sunden[1], M. Cecconello[1], S. Conroy[1], G. Ericsson[1], M. Gatu Johnson[1], S.D. Pinches[2], S.E. Sharapov[2], M. Weiszflog[1] and JET EFDA contributors*

JET-EFDA, Culham Science Centre, OX14 3DB, Abingdon, UK

[1]EURATOM-VR, Dept. of Physics and Astronomy, Uppsala University, Sweden
[2]EURATOM-CCFE Fusion Association, Culham Science Centre, OX14 3DB, Abingdon, OXON, UK
** See annex of F. Romanelli et al, "Overview of JET Results",*
(23rd IAEA Fusion Energy Conference, Daejon, Republic of Korea (2010)).

Preprint of Paper to be submitted for publication in
Plasma Physics and Controlled Fusion

ABSTRACT

When analysing data from fast ion measurements it is normally assumed that the Larmor radii of the energetic ions are small compared to the width of the field of view of the measuring instrument. It is demonstrated here that this approximation is not always valid, by analyzing neutron emission spectrometry data from a JET experiment with deuterium neutral beams together with radiofrequency heating at the 3rd harmonic of the deuterium cyclotron frequency. In the experiment, the neutron time-of-flight spectrometer TOFOR was used to measure the neutrons from the d(d,n)^{3}He-reaction. Comparison of the experimental data with Monte Carlo calculations shows that the Larmor gyration of the fast ions needs to be included in the modelling to get a good description of the data. Similar effects are likely to be important for other fast ion diagnostics, such as γ-ray spectroscopy and neutral particle analysis, as well.

1. INTRODUCTION

It is important to understand the behaviour of fast, supra thermal particles in magnetic confinement fusion devices, since a future burning plasma relies on the self heating from the fast 3.5 MeV α-particles produced in the d(t,n)^{4}He reaction. In present day devices, this self heating is mimicked by producing fast ions with the external heating systems: the neutral beam injector (NBI) and the ion cyclotron resonance heating (ICRH). Of great concern is the ability to confine the fast ions until they have transferred their energy to the bulk plasma. Loss of confinement would lead to impaired heating efficiency, as well as undesirable heat loads on the reactor walls [1]. Fast ions are also able to stabilize as well as drive magnetohydrodynamic (MHD) instabilities in the plasma [1]. This interplay with MHD activity can lead to redistribution or losses of fast ions [2].

Neutron emission spectrometry (NES) provides one way of diagnosing fast ions [3, 4]. The energy of a fusion neutron depends on the velocities of the reacting ions, and hence a neutron energy spectrum contains information about the reactant velocity distribution. In this paper the neutron emission from the d(d,n)^{3}He reaction is studied, and the neutron spectrum therefore probes the deuterium distribution in the plasma.

An important part in the analysis of NES data is the ability to calculate neutron spectra. The neutron spectrum can be obtained by integrating given velocity distributions of the reactants over the relevant cross section. This approach was followed e.g. in [4], where the neutron emission calculated from distributions obtained with the NBI modelling code NUBEAM [5] was compared with NES data. It is also possible to use this technique in the opposite direction, i.e. to estimate the fast ion distribution from measured data [3].

In references [3, 4], neutron spectra are calculated using Monte Carlo techniques, and there is an implicit averaging over the Larmor gyration of the ions associated with the calculations. However, if the plasma contains ions with Larmor radii comparable to the field of view of the spectrometer, the gyro motion of a particular ion can take place partly outside the field of view and the averaging

may not be valid. This can cause discrepancies between calculated and measured spectra.

The aim of the work presented in this paper is to investigate and model these effects for the neutron spectrometer TOFOR at the JET tokamak. TOFOR data from an experiment using ICRH tuned to the 3rd harmonic of the cyclotron frequency of deuterium, together with deuterium neutral beams, was studied. This heating scheme creates fast deuterons in the MeV range, which means that their Larmor radii are comparable to the width of the field of view of TOFOR. At these energies the d(d,n)^{3}He cross section is several orders of magnitude larger than at thermal energies and thus the neutron spectrum will be dominated by neutrons produced in reactions involving the fast ions. Furthermore, the ICRH resonance layer coincided with the outer edge of the field of view of TOFOR, causing the fast ion distribution to be strongly peaked around this region in the plasma. Therefore, the large Larmor radii (LLR) of the fast ions are likely to be important for TOFOR measurements in this experiment.

These LLR effects were first observed in [6] for neutron spectrometry and were also used in [7] in the analysis of γ-ray spectroscopy data. The work presented here aims to investigate these effects in a systematic manner.

The paper is organized as follows. In section 2 it is reviewed how harmonic ICRH creates a non-Maxwellian fast ion population in the plasma, and a model that takes LLR effects into account in the calculation of neutron spectra is described. Section 3 describes the TOFOR spectrometer and the JET experiment under consideration. A comparison between calculated spectra and TOFOR data is presented in section 4, section 5 is devoted to the discussion and interpretation of the results and conclusions are presented in section 6.

2. MODELLING THE NEUTRON EMISSION FROM FAST ION REACTIONS

2.1. HARMONIC RF HEATING

Radiofrequency heating of a plasma at a harmonic of the ion cyclotron frequency is a finite Larmor radius effect and therefore works better if there are energetic ions to couple to. In the JET discharges considered in this paper, the ICRH was tuned to the 3rd harmonic of the deuterium cyclotron frequency, and deuterium NBI was used to provide a seed of energetic ions for the ICRH. The energy of the NBI ions was around 100 keV. These ions were then accelerated up to energies in the MeV range by the ICRH [3].

The energy distribution f_{fast} of the fast ions produced by the auxiliary heating can be calculated from a Fokker-Planck equation derived in [8]. The solution is the steady-state distribution for a homogeneous plasma with prescribed values for the ICRH and NBI power absorbed per unit volume. The energy distribution obtained in this way was previously used for neutron spectrometry analysis in [3] and [9]. A typical fast fuel ion distribution, f_{fast}, arising from 3rd harmonic ICRH and NBI heating is shown in figure 2. This distribution corresponds to a plasma with density $3 \cdot 10^{19}$ m^{-3}, heated with 0.5 MW/m^3 of ICRH and 110 keV NBI with the intensity $1 \cdot 10^{19}$ m^{-3}s^{-1}. The

distribution has a non-Maxwellian tail, extending up to several MeV. Above a certain energy, E^*, the distribution function drops rapidly. In the approximation of cold plasma theory, E^* scales as [10]

$$E^* \propto \frac{B^2}{n_e}, \tag{1}$$

where B is the magnetic field strength and n_e is the electron density.

In addition to the energy distribution, further information about the fast ion distribution can be obtained by considering the ions normalized magnetic moment Λ defined as

$$\Lambda = \frac{\mu B_0}{E}, \tag{2}$$

where μ is the magnetic moment, E is the kinetic energy and B_0 the toroidal field at the magnetic axis R_0. The kinetic energy and the magnetic moment are invariants of motion; E and Λ are conserved for an ion moving in the magnetic field of the tokamak. When energy is added to the plasma by means of the external heating systems, the invariants change. If an ion gains energy ΔE through interaction with the ICRH wave field of angular frequency ω the corresponding change in Λ is [11]

$$\Delta\Lambda = \left(\frac{n\omega_{c0}}{\omega} - \Lambda\right)\frac{\Delta E}{E + \Delta E}, \tag{3}$$

where ω_{c0} is the ion cyclotron frequency at the magnetic axis and $n = 1, 2, 3, \ldots$ is the harmonic number of the ICRH.

Mainly the perpendicular component of the ion velocity is accelerated by the ICRH, which means that the fast ions created in this way will generally be trapped particles. In a large aspect ratio tokamak, where the magnetic field behaves approximately as $1/R$, Λ for such a particle can be expressed in terms of its turning point R_{tp}

$$\Lambda \approx \frac{R_{tp}}{R_0}. \tag{4}$$

Thus, from (3) and (4) it follows that the turning points of ions interacting with the ICRH wave field is driven towards the resonance position

$$R_{res} = R_0\frac{n\omega_{c0}}{\omega}. \tag{5}$$

The higher energy the particle gets the shorter the distance between the turning point and the resonance.

The above equations are for a single particle interacting with one wave mode; collisions between the plasma particles will further add to the picture. At low energies pitch angle scattering dominates, which will tend to flatten the Λ-distribution. Above the so called critical energy

$$E_{crit} = \left(\frac{3\sqrt{\pi}}{4}\right)^{2/3}\left(\frac{m_i}{m_e}\right)^{1/3} T_e \tag{6}$$

electron drag becomes the more important factor. Since the pitch angle is only weakly affected by

electron drag becomes the more important factor. Since the pitch angle is only weakly affected by these collisions, ions above E_{crit} will to a first approximation follow the characteristic lines in the (Λ, E)-plane described by (3). This is illustrated in figure 3a for different initial values of Λ.

The Λ-distribution is strongly peaked around $\Lambda_{res} = n\omega_{c0}/\omega$ which means that ions with energies larger than about 500 keV will generally be trapped, and have their turning points close to the resonance position. An example of such an ion orbit is shown in figure 3b. It is seen that only a part of the Larmor gyration is inside the field of view of TOFOR. This will affect the shape of the neutron spectrum as described in section 2.2 below.

In the vicinity of the turning point the parallel velocity of the ions is close to zero, i.e. the pitch angles are close to 90°. Hence, fast ions will spend most of their time near the turning points in the resonance layer. For a scenario with high ICRH power there will therefore be a large population of energetic ions close to the resonance layer, whereas in the rest of the plasma the fraction of fast ions will be much lower. This narrow region of fast particles with pitch angles close to 90° will be referred to as the fast particle region in what follows.

From figure 3a it is seen that the spread in Λ is typically less than 0.1 for ion energies above 500 keV. From 4, this corresponds to turning points distributed within a few decimetres around the resonance position (assuming $R_{res} \approx 3$ m). Experience from the ICRH modelling code SELFO [12] also suggests that this is indeed the typical width of the fast particle region for the type of plasma scenario considered here [13].

2.2. CALCULATIONS OF NEUTRON ENERGY SPECTRA

In a fusion reaction producing a neutron and a residual product of mass m_r, the neutron energy is given by [14]

$$E_n = \frac{1}{2} m_n v_{cm}^2 + \frac{m_r}{m_n + m_r}(Q + K) + v_{cm}\cos\theta\sqrt{\frac{2m_n m_r}{m_n + m_r}(Q + K)}, \tag{7}$$

where m_n is the neutron mass, v_{cm} the centre of mass speed, Q the released fusion energy, and K is the relative kinetic energy of the reactants. θ is the angle between the centre of mass velocity and the neutron emission direction in the centre of mass frame. To calculate the neutron energy spectrum from two fuel ion distributions f_i and f_j one needs to evaluate an integral of the following type:

$$\frac{dN}{dE} = \frac{1}{1 + \delta_{ij}} \int_{\mathbf{r}} \int_{\mathbf{v}_i} \int_{\mathbf{v}_j} f_i(\mathbf{v}_i, \mathbf{r})\, f_j(\mathbf{v}_j, \mathbf{r})\, \delta(E - E_n)\, v_{rel} \frac{d\sigma}{d\Omega}(\mathbf{v}_{rel})\, \Delta\Omega(\mathbf{r})\, d\mathbf{r} d\mathbf{v}_i d\mathbf{v}_j. \tag{8}$$

Here, $\mathbf{v}_{rel} = \mathbf{v}_i - \mathbf{v}_j$ is the relative velocity between the colliding fuel ions and $d\sigma/d\Omega$ is the differential cross section of the reaction. The quantity $\Delta\Omega(\mathbf{r})$ is the solid angle of detector area seen from the position $\mathbf{r}$ in the plasma.

The Larmor motion of fast ions is strongly reflected in the neutron spectrum. Consider the radial neutron emission arising from a mono-energetic fast ion distribution ($E \gg kT_{plasma}$) reacting with

the thermal background plasma in a JET-like tokamak. Due to variation along the ion orbit of the $\cos\theta$-term in (7), the neutron spectrum will be double-humped, with energies ranging between $E_{n,min}$ and $E_{n,max}$, as illustrated in figure 4a. However, if part of the orbit is invisible for some reason, the observed neutron spectrum will change. Figure 4b shows how the low energy side of the spectrum is reduced if the down going part of the orbit is not seen by the measuring instrument.

The localization of fast ions to a narrow region in the plasma is believed to impact the results of fast ion measurements in precisely this way, if the field of view overlaps the fast particle region. In the experiment considered in this paper, the fast ions will move along orbits similar to the one in figure 3b, where it can be seen that only a fraction of the Larmor gyration is visible to TOFOR, thus leading to a situation similar to the one illustrated in figure 4b.

To investigate this effect, (8) was evaluated with a Monte Carlo calculation sampling the two velocity distributions f_i and f_j, representing the thermal background plasma and the fast deuterium ions, respectively. The fast ions were assumed to occur only inside the fast particle region, close to the ICRH resonance layer. The fast ion energy distribution f_{fast} was obtained from the 1D Fokker-Planck equation as described in section 2.1. Measured values of electron density, temperature and heating powers are used as input for this calculation. Since it is necessary to specify the power density of the ICRH and the NBI, an assumption must also be made on the volume of the plasma that absorbs the injected power. In all the simulations in this paper the absorbing volumes were set to 7 m^3 and 10 m^3, for ICRH and NBI respectively.

The neutron energy spectrum, including LLR effects, can now be calculated in the following sequence of steps:

1. Sample fast particle energies from f_{fast}, along with positions of their gyro centres, which are assumed to be uniformly distributed in the fast particle region. In all the simulations the fast particle region is assumed to be between $R = 2.93$ m and $R = 3.15$ m, in line with the discussion in section 2.1.

2. Calculate the particle velocities by using random values for the gyro phase and assuming the cosine of the pitch angles to be uniformly distributed in the interval $\cos(90^\circ \pm 10^\circ)$, (c.f. the discussion in section 2.1).

3. Calculate the Larmor radii and the positions of the particles. If the particle happens to be inside the field of view, the neutron energy – for a neutron emitted towards TOFOR – arising from a reaction between the fast ion and the bulk plasma is calculated and included in the spectrum, weighted with the corresponding cross section according to (8).

3. EXPERIMENTAL

3.1. THE TOFOR NEUTRON SPECTROMETER

The neutron energy spectra during the experiment were measured with the TOFOR spectrometer

[15]. This is a time-of-flight spectrometer that measures neutron energies by recording the time required for neutrons to travel between two sets of scintillator detectors, S1 and S2. In order to be detected in S2, the scattering angle in S1 needs to be about 30 degrees. The flight time t_{TOF} of a neutron scattered in S1 can be related to the energy of the incoming neutron

$$E_n = \frac{2m_n r^2}{t_{TOF}^2}, \tag{9}$$

where r is the radius of the sphere that would precisely touch both of the detector sets. A neutron energy of 2.5 MeV corresponds to a t_{TOF} of 65 ns, and 14 MeV corresponds to 27 ns.

TOFOR is situated in the roof laboratory above the JET torus hall, as shown in figure 5, and the distance to the torus mid plane is about 19 m. The line of sight of TOFOR is described in detail in [16]. The solid angle of the detector seen from the plasma mid plane is shown in figure 6. $\Delta\Omega$ is largest at $R = 2.88$ m, and falls off symmetrically on both sides, due to the shadowing of the collimator. The inner and outer limits are located at 2.74 m and 3.02 m respectively.

3.2. THE JET EXPERIMENT

Neutron spectra were calculated for an experiment conducted at JET during the fall of 2008. Discharges with pulse numbers in the range 74937 to 74951, that used ICRH tuned to the 3rd harmonic of the deuterium cyclotron frequency, together with 100 keV deuterium NBI, were studied. The harmonic RF heating couples efficiently to energetic beam ions in the resonance layer and creates non-Maxwellian fast ion distributions, see figure 2 for an example. In the pulses considered here, both the NBI and the ICRH delivered around 3-4 MW of heating power and the frequency of the ICRH was 51.5 MHz. The toroidal magnetic field B_0 varied between 2.25 and 2.3 T, placing the resonance position R_{res} at about $R = 3$ meters. This is very close to the outer limit of the field of view of TOFOR. Time traces of the applied auxiliary heating power for three of the discharges in the experiment are shown in figure 7. Also shown is the central electron temperature and density, obtained from electron cyclotron emission and LIDAR measurements respectively.

4. RESULTS

Calculated spectra for a number of different time intervals during different JET discharges are presented in figure 8. Each calculated spectrum is the sum of two components. One is the result of the reaction between the fast ion distribution, f_{fast}, and the bulk plasma, as described in section 2.2, and the other one is a so called backscatter component [16], that takes into account neutrons scattering off the reactors far wall and into the field of view of the TOFOR spectrometer. Only the sum of the two components is shown, for clarity. One should note in figure 8 that the high energy (short time-of-flight) cut-off in the spectra is not always correctly reproduced in the calculations. This could e.g. be due to uncertainties in the LIDAR measurements of the electron density, since E^* is inversely proportional to this quantity (see section 2.1).

Two kinds of spectra were calculated. One including the LLR effects (called LLR spectrum in what follows) as described in section refspectra, and one where the LLR effects are not considered (called gyro centre spectrum), i.e. all the neutrons are assumed to be emitted from the gyro centres of the fast ions.

The spectra are shown both on a neutron energy scale and on the corresponding time-of-flight scale. In the latter case the spectra have been folded with the TOFOR response function [15], and are fitted to TOFOR data together with the backscatter component, with a Bayesian analysis. It should be noted that the intensities of the two spectral components are the only free parameters in the fit. For the gyro centre spectra, the fit is restricted to the region $t_{TOF} < 55$ ns, in order to facilitate the comparison between the different spectra. However, when comparing the reduced χ^2-values for the different fits (see below) the full time-of-flight range is used for both the LLR and the gyro centre spectra.

The intensity of the backscatter component is subject to a Bayesian prior at 17% of the direct neutron emission. This is known to be the typical intensity of backscatter emission from previous NES analysis [16].

The most striking feature about the calculated spectra is the much larger intensity of low energy (long time-of-flight) neutrons that is evident in all the gyro centre spectra compared to the LLR spectra. Clearly, the calculated LLR spectra follow the data much more closely over the entire energy range.

In addition to the neutron spectra shown in figure 8, spectra were calculated for a number of time slices for all the successful discharges from the experiment session under consideration. Each spectrum was fitted to the corresponding TOFOR data and the reduced χ^2 for the gyro centre spectra, χ^2_0, were compared with the reduced χ^2 for the LLR spectra, χ^2_{LLR}. A total of 31 time slices were analyzed, for discharges in the range 74937 to 74951. χ^2_{LLR} is significantly lower than χ^2_0 for all the cases studied. For 20 out of the 31 time slices χ^2_{LLR} is less than 2, whereas χ^2_0 never goes below 6. However, in a few cases the fit is quite poor even when including the LLR effects. One example is discharge number 74937 at t = 15-15.5 s, which is shown in figure 8. For this case $\chi^2_{LLR} = 9.7$, and the fit is clearly not satisfactory. The reason for the poor fits is discussed further in the next section.

5. DISCUSSION

It is evident from the results in figure 8 that the calculated neutron spectra describe the experimental data better when LLR effects are taken into account. The fact that the low energy (long time-of-flight) side of the spectrum is overestimated in the gyro centre spectra is expected for the plasma scenario under consideration; since the resonance layer is close to the outboard part of the field of view of TOFOR, fast ions travelling *a*way from the detector will more often be outside the field of view compared to neutrons travelling *t*owards it. Neutrons produced in reactions during the downward part of an ion orbit will be down shifted in energy due to the $\cos\theta$-term in (7).

Therefore the calculated spectrum contains too many low energy neutrons if LLR effects are not taken into account.

In order to quantify the importance of the LLR effects we introduce the LLR index, α_{LLR}, as the ratio between the Larmor orbit width of fast ions with a given energy, E_{ion}, and the width of the field of view of a certain measuring instrument, Γ_{inst}. This gives

$$\alpha_{LLR} = \sqrt{\frac{2}{3}} \frac{\sqrt{m_{ion} E_{ion}}}{Z \Gamma_{inst} B}, \tag{10}$$

where m_{ion} is the mass in MeV/c^2, Z is the atomic number of the ions and B is the magnetic field in Tesla. E_{ion} should be given in MeV and Γ_{inst} in centimetres. $\alpha_{LLR} = 1$ means that an ion with a pitch angle of 60° will have a Larmor orbit width equal to Γ_{inst}. Hence, if α_{LLR} is of order unity or larger for a particular instrument, LLR effects could be important. For the experiment considered in this paper, with $E_{ion} \sim 1$ MeV and $\Gamma_{TOFOR} = 28$ cm, Γ_{LLR} becomes 0.6. However, in addition to a LLR index of order unity, it is also necessary that the spatial distribution of fast ions changes appreciably inside the field of view, otherwise the LLR effect will cancel out. In this experiment, the anisotropy was created by the ICRH (c.f. the (Λ, E)-distribution in figure 3a).

It should be noted that the importance of the LLR effect is exceptionally large in the discharges considered here. The fast deuterium tail extending up to several MeV, in combination with the high d(d,n)^{3}He cross section at these energies, make neutrons from fast ion reactions completely dominate the energy spectrum. Also, the location of the resonance layer just at the outer edge of the field of view of TOFOR creates a steep gradient in the spatial distribution of the fast ions. For a different plasma scenario where the neutron emission is dominated by reaction from ions with smaller Larmor radii, such as plasmas heated with 100 keV NBI only ($\alpha_{LLR} \approx 0.2$), or ohmic plasmas ($\alpha_{LLR} \approx 0.1$), LLR effects do not affect neutron spectrometry measurements.

Magnetohydrodynamic (MHD) activity, such as toroidal Alfvn eigenmodes and monster sawteeth, was observed in most of the pulses studied in this paper. The redistribution of fast particles due to MHD activity has been seen to affect the detailed shape of the high energy part of the neutron spectrum [3], but on a much smaller scale compared to the typical difference between the LLR and gyro centre spectra. No clear correlation between the presence of MHD activity and the quality of the fit for a given time-slice could be seen. The reason for the poor fits for some time slices can be attributed to the limitations of the ICRH model, as discussed below.

5.1. LIMITATIONS OF THE ICRH MODEL

The model for the fast ion distribution used in this paper provides a quick and simple way to capture the physics of relevance for the neutron emission from the discharges under consideration, such as the cut-off energy E^*, the non-Maxwellian tail and the location of turning points close to the resonance position. Its computational simplicity makes it suitable for the kind of study presented here, where the aim was to investigate the LLR effects for a large number of time slices and plasma discharges. However, since the model is not self consistent and does not fully consider

the geometry and profile of the plasma, it is not surprising that the calculated neutron spectrum does not describe the data perfectly for all the cases studied.

As pointed out in section 2.1, the energy distribution f_{fast} is the steady-state solution of the Fokker-Planck equation. Hence, if the plasma parameters vary significantly during the time slice under consideration the calculated energy distribution may be inaccurate. As an example, consider the electron density, which is inversely proportional to the cut-off energy E^* according to (1). As seen from figure 7, the density changes from $3 \cdot 10^{19}$ to $4 \cdot 10^{19}$ m^{-3} between $t = 14$-16 s in discharge 74937. This lowers the calculated E^* and thereby the cut-off in the calculated neutron spectrum. In reality the fast ions are not likely to respond this quickly to the density change, which is why the fit for $t = 15 - 15.5$ s is quite poor even when including the LLR effects (see figure 8).

By the same reasoning, the 5 percent uncertainty associated with the LIDAR measurement of the central electron density could also explain some of the discrepancies between the calculated and the measured neutron spectra.

Very few assumptions about plasma parameters have been made in order to reach the results presented above. Densities, temperatures, heating powers etc., are all measured quantities from their respective diagnostics at JET. However, as described in section 2.2, an assumption was made about the volume of the plasma that absorbs the injected power. No attempt was made to estimate these parameters from the underlying physics, the volumes were adjusted to give good fits for as many time slices as possible.

It is possible to obtain better fits by fine tuning the absorbing volumes for each individual time-slice. Another possibility is to vary the inner edge of the fast particle region, thereby changing the details in the shape of the low energy side of the neutron spectrum. By adjusting these two parameters it is possible improve the fits for several of the time slices that was studied. This approach has not been pursued in this paper, since it is of little interest to fine tune the parameters of a model that is only meant to capture the gross features of the fast ion distribution. However, if the model presented in this paper could be used to analyze fast ion data from some other diagnostic it would be of interest to compare the values of these parameters.

6. SUMMARY AND CONCLUSION

Neutron energy spectra from 3rd harmonic ICRH and NBI heated plasmas have been measured using the TOFOR neutron spectrometer at JET. The data analysis indicates that the details in the field of view of the detector need to be taken into account in order to fully understand the shapes of the measured neutron spectra. This is because the Larmor radii of the fast fuel ions at the ICRH resonance are comparable to the width of the field of view.

A model taking this effect into consideration has been developed, and is applied when modelling the neutron emission in the above analysis. The result is a much better agreement with experimental data, than if LLR effects are not considered. The differences between calculated spectra with and without corrections for the finite Larmor radius agree with what one expects from the physics of ICRH and fast ions and the relevant kinematics.

The conclusion is therefore that LLR effects can be of great importance for the interpretation of fast ion measurements. In order to quantify the importance for a given instrument and plasma scenario, a LLR index was introduced. A LLR index of order unity means that the Larmor radii of the fast ions are comparable to the width of the field of view of the measuring instrument. If this condition is fulfilled and the fast ion distribution is anisotropic in the field of view of the instrument, LLR effects are likely to impact the fast ion measurement.

ACKNOWLEDGMENTS

The authors acknowledge the discussions with Dr. Thomas Johnson about ICRH physics. This work was supported by EURATOM and carried out within the framework of the European Fusion Development Agreement. The views and opinions expressed herein do not necessarily reflect those of the European Commission.

REFERENCES

[1]. ITER Physics Basis 1999 Nuclear Fusion **39** 2471 10
[2]. Sharapov S.E. et al 2005 Nuclear Fusion **45** 1168
[3]. Hellesen C. et al 2010 Nuclear Fusion **50** 022001
[4]. Hellesen C. et al 2010 Plasma Physics and Controlled Fusion **52** 085013
[5]. Pankin A. 2004 Computer Physics Communications **159** 157
[6]. Eriksson J. 2010 Diploma Thesis, Uppsala University http://urn.kb.se/resolve?urn=urn:nbn:se:uu:diva-120425
[7]. Tardocchi M. et al 2010 Europhysics Conference Abstracts **34A** O4.119
[8]. Stix T.H. 1975 Nuclear Fusion **15** 737
[9]. Gatu Johnson M. et al 2010 Review of Scientific Instruments **81** 10D336
[10]. Salmi A. et al 2006 Plasma Physics ans Controlled Fusion **48** 717
[11]. Eriksson L-G. et al Physics of Plasmas **6** 513

[12]. Hedin J. et al 2002 Nuclear Fusion **42** 527
[13]. Johnson T. KTH Royal Institute of Technology private communication
[14]. Brysk H. 1973 Plasma Physics **15** 611
[15]. Gatu Johnson M. et al 2008 Nuclear Instruments and Methods A **591** 417
[16]. Gatu Johnson M. et al 2010 Plasma Physics and Controlled Fusion **52** 085002

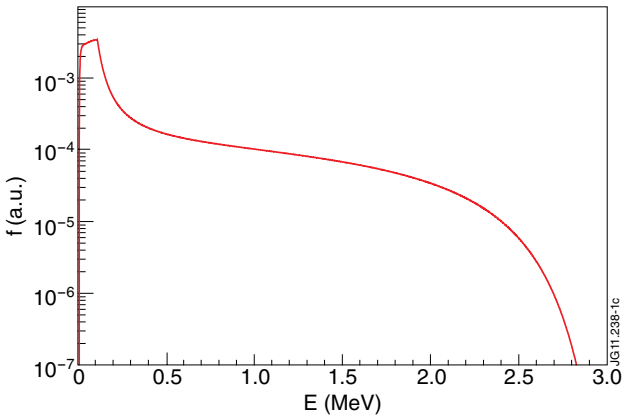

Figure 1: An example of a fast deuterium energy distribution, f_{fast}, produced by 3rd harmonic ICRH and deuterium NBI.

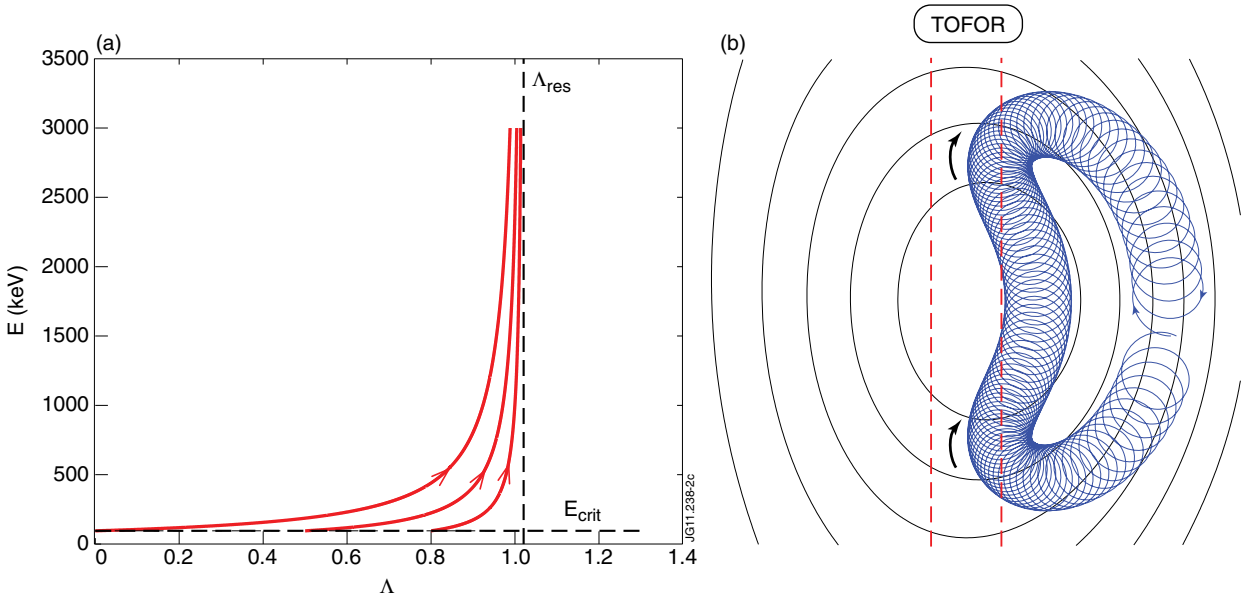

Figure 2: (a) Characteristic lines in the (Λ, E)-plane followed by ions above E_{crit}, for an example with 3rd harmonic ICRH on deuterium. The electron temperature is assumed to be 5keV, giving E_{crit} = 95keV. (b) A typical orbit from this (Λ, E)-distribution (E = 2MeV, Λ = 1). The field of view of TOFOR is indicated with dashed lines.

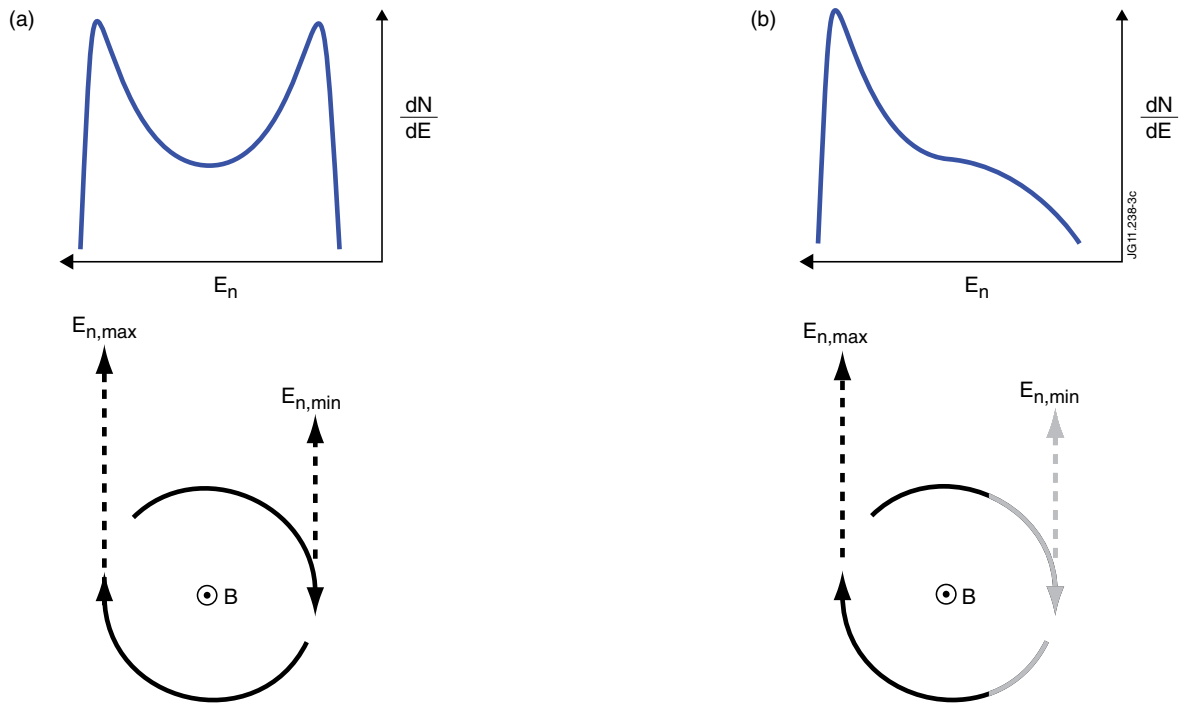

Figure 3: (a) A typical double-humped spectrum arising from a mono-energetic fast ion distribution. (b) If the down going part of the orbit is shadowed, the low energy part of the spectrum is reduced. Note the reversed scale on the energy axes.

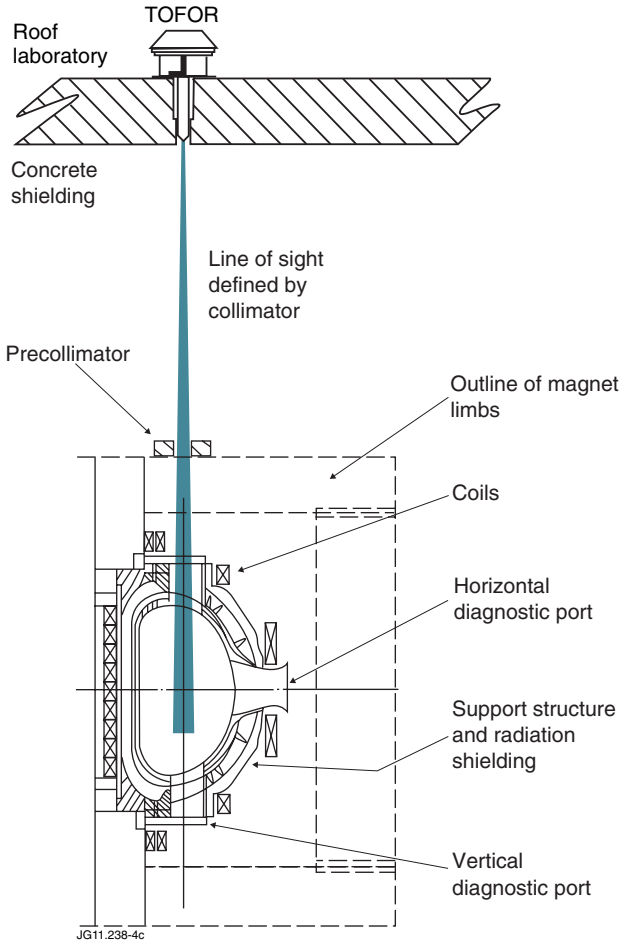

Figure 4: The location of TOFOR in the JET roof laboratory above the torus hall (not to scale).

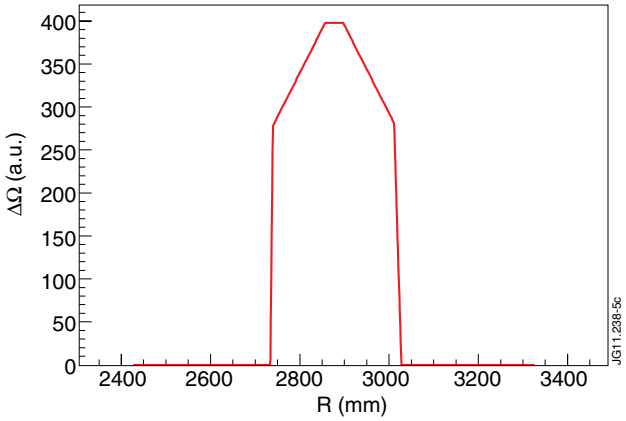

Figure 5: The solid angle of the detector seen from the plasma mid plane as a function of the radial coordinate R.

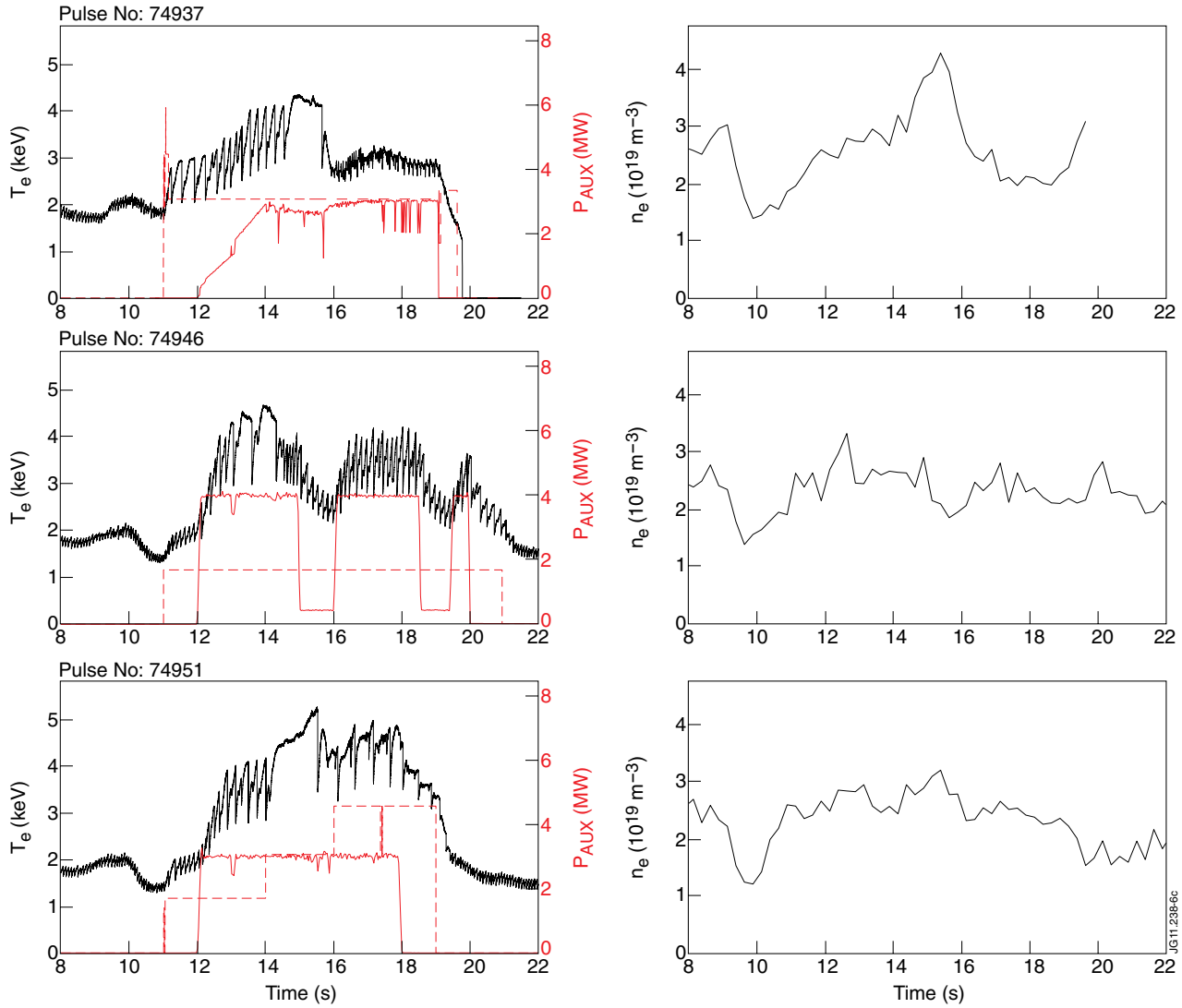

Figure 6: Key plasma parameters as function of time for JET Pulse No's: 74937, 74946 and 74951. Left column: central electron temperature Te (black solid line), auxiliary heating power P_{AUX} (NBI as dashed red line and ICRH as solid red line). Right column: core electron density ne (black solid line).

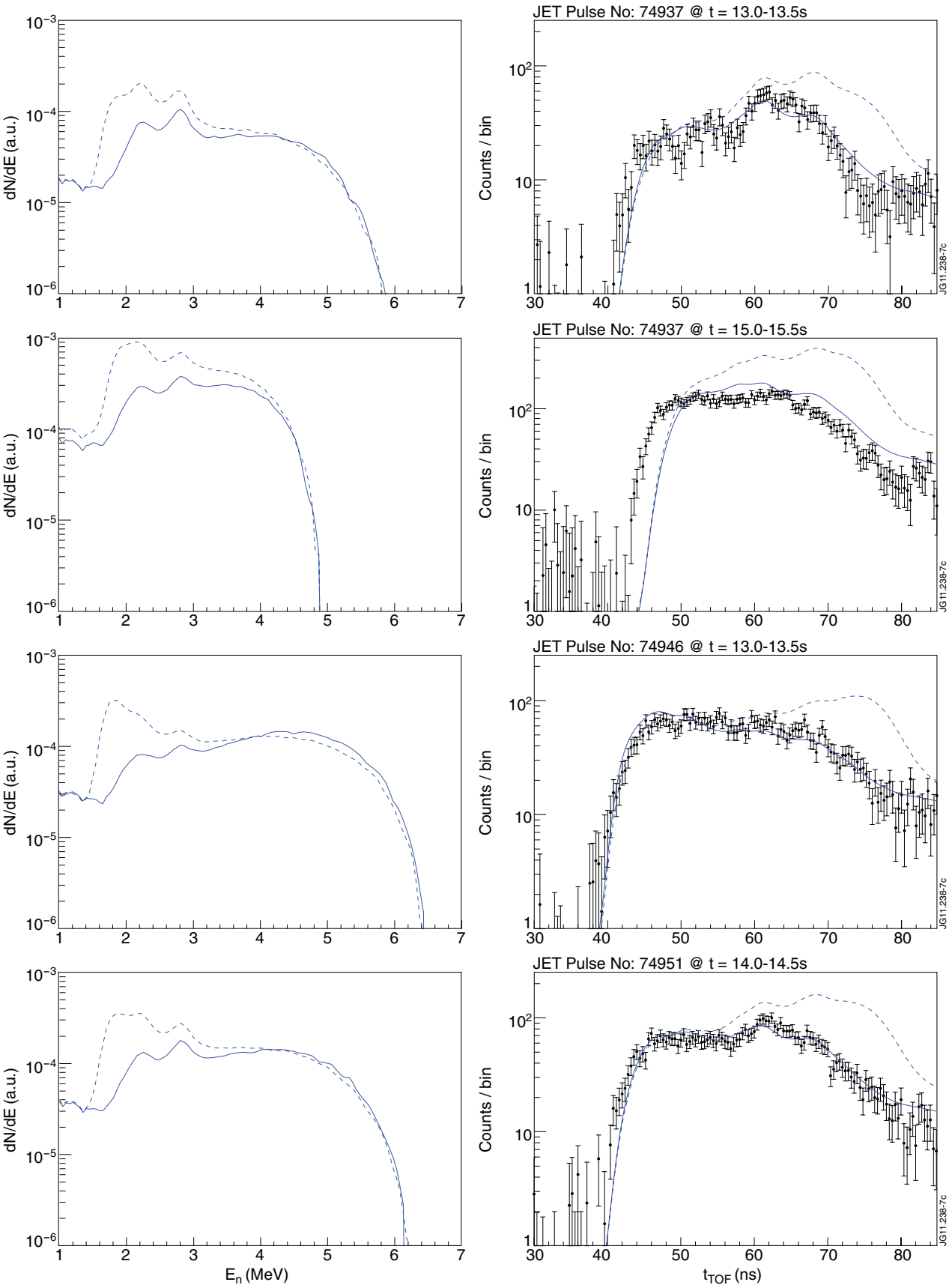

Figure 7: The left column shows neutron energy spectra calculated taking LLR effects into account (solid line), and without taking LLR effects into account (dashed line). In the right column the spectra have been folded with the response function of TOFOR and are fitted to TOFOR data (points with error bars). The calculated spectra are seen to overestimate the experimental data for low energies (long time-of-flights) if LLR effects are not taken into account in the calculations.